

PAPER

Performance Comparison between CDTD and STTD for DS-CDMA/MMSE-FDE with Frequency-Domain ICI Cancellation

Kazuaki TAKEDA^{†a)}, Member, Yohei KOJIMA[†], Student Member, and Fumiyuki ADACHI[†], Fellow

SUMMARY Frequency-domain equalization (FDE) based on the minimum mean square error (MMSE) criterion can provide a better bit error rate (BER) performance than rake combining. However, the residual inter-chip interference (ICI) is produced after MMSE-FDE and this degrades the BER performance. Recently, we showed that frequency-domain ICI cancellation can bring the BER performance close to the theoretical lower bound. To further improve the BER performance, transmit antenna diversity technique is effective. Cyclic delay transmit diversity (CDTD) can increase the number of equivalent paths and hence achieve a large frequency diversity gain. Space-time transmit diversity (STTD) can obtain antenna diversity gain due to the space-time coding and achieve a better BER performance than CDTD. Objective of this paper is to show that the BER performance degradation of CDTD is mainly due to the residual ICI and that the introduction of ICI cancellation gives almost the same BER performance as STTD. This study provides a very important result that CDTD has a great advantage of providing a higher throughput than STTD. This is confirmed by computer simulation. The computer simulation results show that CDTD can achieve higher throughput than STTD when ICI cancellation is introduced.

key words: DS-CDMA, MMSE-FDE, cyclic delay transmit diversity (CDTD), space-time transmit diversity (STTD), ICI cancellation

1. Introduction

With the growing market of mobile wireless communications, high-rate data services are demanded. Wireless channels for such high-speed data transmissions are severely frequency-selective [1], and this degrades the transmission performance significantly. In the present mobile communication systems which offer data services of a few Mbps, direct sequence code division multiple access (DS-CDMA) has been adopted to exploit a moderate channel frequency-selectivity by using rake combining [2], [3]. However, for much higher-rate data transmissions than the present systems, the wireless channels become severely frequency-selective and hence, the bit error rate (BER) performance of rake combining significantly deteriorates due to the strong inter-path interference (IPI). Therefore, an advanced equalization technique is necessary.

Frequency-domain equalization (FDE) based on the minimum mean square error (MMSE) criterion can improve the BER performance of DS-CDMA transmissions [4]–[7].

However, the residual inter-chip interference (ICI) is present after MMSE-FDE and this limits the BER performance improvement. The frequency-domain interference cancellation was proposed for DS-CDMA uplink in [8]. Recently, we proposed a frequency-domain ICI cancellation for the DS-CDMA downlink and showed that frequency-domain ICI cancellation can bring the BER performance very close to the theoretical lower-bound [9].

To further improve the BER performance, transmit antenna diversity technique is effective. In this paper, we assume a DS-CDMA/MMSE-FDE system with multiple transmit antennas and single receive antenna. Recently, cyclic delay transmit diversity (CDTD) has been proposed for multi-carrier transmissions [10]. CDTD increases the number of equivalent paths by transmitting the same data block from different antennas after adding different cyclic delays, and hence can achieve a large frequency diversity gain. CDTD can also be applied to DS-CDMA/MMSE-FDE and can improve the BER performance in a weak frequency-selective fading channel [10]. Space-time transmit diversity (STTD) is another attractive transmit diversity technique which obtains the antenna diversity gain owing to the space-time coding [11]. It was reported [12] that the performance improvement obtained by CDTD is smaller than STTD. This is the case when an ICI cancellation technique is not used. Some literature on CDTD can be found for single-carrier transmission or DS-CDMA with FDE [12], [13]; however, the ICI cancellation was not considered.

Objective of this paper is to show that the BER performance degradation of CDTD is mainly due to the residual ICI. We theoretically show that the introduction of ICI cancellation to CDTD provides almost the same BER performance as STTD. This study provides a very important result that CDTD has a great advantage of providing a higher throughput than STTD. STTD using more than two transmit antennas reduces the transmission data rate or throughput. On the other hand, CDTD can use an arbitrary number of transmit antennas without reducing the transmission data rate at all. This suggests that if CDTD with ICI cancellation provides similar BER performance to STTD, CDTD will provide a higher throughput than STTD. The reason why CDTD can achieve higher throughput than STTD is given below. CDTD relies on the frequency diversity gain while STTD relies on the antenna diversity gain. In CDTD, the same chip-block of N_c chips is simultaneously transmitted

Manuscript received September 8, 2008.

Manuscript revised March 17, 2009.

[†]The authors are with the Department of Electrical and Communication Engineering, Graduate School of Engineering, Tohoku University, Sendai-shi, 980-8579 Japan.

a) E-mail: takeda@mobile.ecei.tohoku.ac.jp

DOI: 10.1587/transcom.E92.B.2882

from different antennas after adding different cyclic delays. The transmission data rate is always kept the same (i.e., the coding rate R is kept unity) irrespective of the number N_t of transmit antennas. On the other hand, in the case of STTD, R depends on N_t . When $N_t = 2$, a sequence of 2 chip-blocks is space-time (ST) encoded into 2 parallel sequences of 2 chip-blocks each. Therefore, $R = 1$ as in CDTD. However, when $N_t = 4$, a sequence of 3 chip-blocks is ST encoded into 4 parallel sequences of 4 chip-blocks each. Therefore, R is reduced to $3/4$. This reduces the achievable throughput of STTD compared to CDTD. Hence, CDTD can remain as a very attractive transmit diversity technique for the down-link (base-to-mobile) application. Furthermore, CDTD has a very simple transmitter structure.

The remainder of the paper is organized as follows. Sections 2 and 3 present DS-CDMA/MMSE-FDE systems using CDTD and STTD. The residual ICI produced after MMSE-FDE is described in Sect. 4. Section 5 presents the ICI cancellation for DS-CDMA/MMSE-FDE using CDTD and STTD. Assuming perfect ICI cancellation, the BER approaches its lower-bound. The theoretical lower-bound can be derived using the signal-to-noise power ratio (SNR). It is shown in Sect. 6 that the same SNR is obtained for CDTD and STTD. In Sect. 7, the BER performances of CDTD and STTD are evaluated by computer simulation to confirm that, with ICI cancellation, both CDTD and STTD give almost the same BER performance. Section 8 offers some conclusions.

2. CDTD

2.1 Transmitted Signal

DS-CDMA transmitter using CDTD is illustrated in Fig. 1. Throughout the paper, chip-spaced time representation of the transmitted signals is used. At the transmitter, a binary data sequence is data-modulated and then, serial/parallel (S/P)-converted to U parallel data sequences. The u th data modulated symbol sequence $d_u(m)$, $u = 0 \sim U - 1$ and $m = 0 \sim N_c/SF - 1$, is then spread by multiplying it with an orthogonal spreading sequence $c_u(t)$, where N_c is the FFT window size and SF is the spreading factor. The resultant U chip sequences are code-multiplexed and further multiplied by a common scramble sequence $c_{scr}(t)$ to make the resultant multicode DS-CDMA signal like white-noise. The spread signal chip block $\{s(t); t = 0 \sim N_c - 1\}$ to be transmitted can be expressed, using the equivalent lowpass rep-

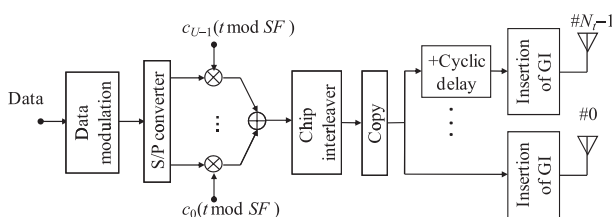


Fig. 1 Transmitter structure using CDTD.

resentation, as

$$s(t) = \left[\sum_{u=0}^{U-1} d_u(\lfloor t/SF \rfloor) \cdot c_u(t \bmod SF) \right] c_{scr}(t), \quad (1)$$

where $\lfloor x \rfloor$ represents the largest integer smaller than or equal to x . In CDTD, the same chip block is simultaneously transmitted from different antennas after adding different cyclic delays [10]. N_t copies of the chip block $\{s(t); t = 0 \sim N_c - 1\}$ are generated and then, cyclic delay $n\Delta$ is added before the transmission from the n th antenna ($n = 0 \sim N_t - 1$) as shown in Fig. 2. The transmission data rate is always the same (i.e., the coding rate R is kept unity) irrespective of the number N_t of transmit antennas. The transmitted chip block from the n th antenna is given by

$$\bar{s}_n(t) = \sqrt{2E_c/N_t T_c} s((t - n\Delta) \bmod N_c), \quad (2)$$

where E_c and T_c denote the chip energy and chip duration, respectively. The transmit signal power is reduced by a factor of N_t to keep the total transmit signal power constant. Finally, the last N_g chips of each block are copied as a cyclic prefix and inserted into the guard interval (GI) placed at the beginning of each block.

2.2 FDE

The GI-inserted chip block is transmitted over a frequency-selective fading channel. The received chip block after the removal of the GI, $\{r(t); t = 0 \sim N_c - 1\}$, is expressed as

$$r(t) = \sum_{n=0}^{N_t-1} \sum_{l=0}^{L-1} h_{n,l} \bar{s}_n((t - \tau_l) \bmod N_c) + \eta(t), \quad (3)$$

where $h_{n,l}$ is the l th ($l = 0 \sim L - 1$) complex-valued path gain between the n th transmit antenna and the receiver with $\sum_{l=0}^{L-1} E[|h_{n,l}|^2] = 1$ ($E[\cdot]$ denotes the ensemble average operation) [14]. We assume block fading where the path gains remain constant over one block length of $(N_c + N_g)$ chips. τ_l is the l th path delay and the maximum time delay τ_{L-1} is assumed to be shorter than the GI. $\eta(t)$ is a zero-mean complex Gaussian process with a variance of $2N_0/T_c$; N_0 is the single-sided power spectrum density of the additive white Gaussian noise (AWGN).

N_c -point fast Fourier transform (FFT) is applied to $\{r(t); t = 0 \sim N_c - 1\}$ to transform it into the frequency-domain signal $\{R(k); k = 0 \sim N_c - 1\}$. $R(k)$ is given by

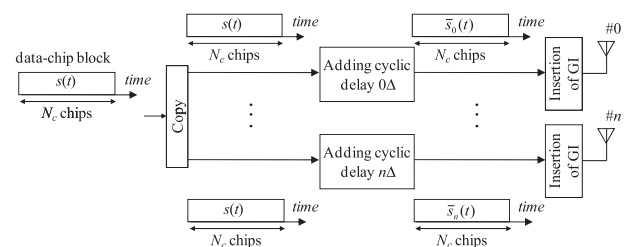


Fig. 2 Procedure of cyclic delay addition.

$$R(k) = \sqrt{2E_c/N_t T_c} H_{CD}(k) S(k) + \Pi(k), \quad (4)$$

where $H_{CD}(k)$, $S(k)$ and $\Pi(k)$ are the channel gain, the k th frequency component of $\{s(t); t = 0 \sim N_c - 1\}$ and the noise due to the AWGN, respectively. H_{CD} and $S(k)$ are given by

$$\begin{cases} S(k) = \sum_{t=0}^{N_c-1} s(t) \exp\left(-j2\pi k \frac{t}{N_c}\right) \\ H_{CD}(k) = \sum_{n=0}^{N_t-1} \sum_{l=0}^{L-1} h_{n,l} \exp\left(-j2\pi k \frac{n\Delta + \tau_l}{N_c}\right). \end{cases} \quad (5)$$

One-tap MMSE-FDE is carried out on $R(k)$ as [7]

$$\begin{aligned} \hat{R}(k) &= R(k)W(k) \\ &= \hat{H}_{CD}(k)S(k) + \hat{\Pi}(k), \end{aligned} \quad (6)$$

where $W(k)$ is the MMSE-FDE weight, $\hat{H}_{CD}(k) = H_{CD}(k)W(k)$ is the equivalent channel gain after MMSE-FDE, and $\hat{\Pi}(k)$ is the noise. $W(k)$ is given by [7]

$$W(k) = \frac{H_{CD}^*(k)}{|H_{CD}(k)|^2 + \left(\frac{1}{N_t} \frac{U}{SF} \frac{E_s}{N_0}\right)^{-1}}, \quad (7)$$

where E_s/N_0 is the symbol energy-to-AWGN power spectrum density ratio. After MMSE-FDE, $\hat{R}(k)$ is transformed by applying N_c -point inverse FFT (IFFT) into the time-domain chip block $\{\tilde{r}(t); t = 0 \sim N_c - 1\}$ as

$$\begin{aligned} \tilde{r}(t) &= \frac{1}{N_c} \sum_{k=0}^{N_c-1} \hat{R}(k) \exp\left(-j2\pi t \frac{k}{N_c}\right) \\ &= \left(\frac{1}{N_c} \sum_{k=0}^{N_c-1} \hat{H}_{CD}(k)\right) s(t) + \mu(t) + \hat{\eta}(t), \end{aligned} \quad (8)$$

where $(1/N_c) \sum_{k=0}^{N_c-1} \hat{H}_{CD}(k)$ is the average equivalent channel gain, $\mu(t)$ is the residual ICI, and $\hat{\eta}(t)$ is the noise [9].

Finally, despreading is performed on $\tilde{r}(t)$, giving

$$\hat{d}_u(m) = \frac{1}{SF} \sum_{t=mSF}^{(m+1)SF-1} \tilde{r}(t) c_u^*(t \bmod SF) c_{scr}^*(t), \quad (9)$$

which is the decision variable associated with $d_u(m)$.

3. STTD

Figure 3 shows the time-domain STTD encoding for $N_t = 2$ and 4. When $N_t = 2$, a sequence of 2 chip-blocks is ST encoded into 2 parallel sequences of 2 chip-blocks each. Therefore, $R = 1$ as in CDTD. However, when $N_t = 4$, a sequence of 3 chip-blocks is ST encoded into 4 parallel sequences of 4 chip-blocks each. Therefore, R is reduced to 3/4. This reduces the achievable throughput of STTD compared to CDTD.

Below, STTD using $N_t = 2$ is considered for simplicity. Even and odd chip blocks are respectively denoted by

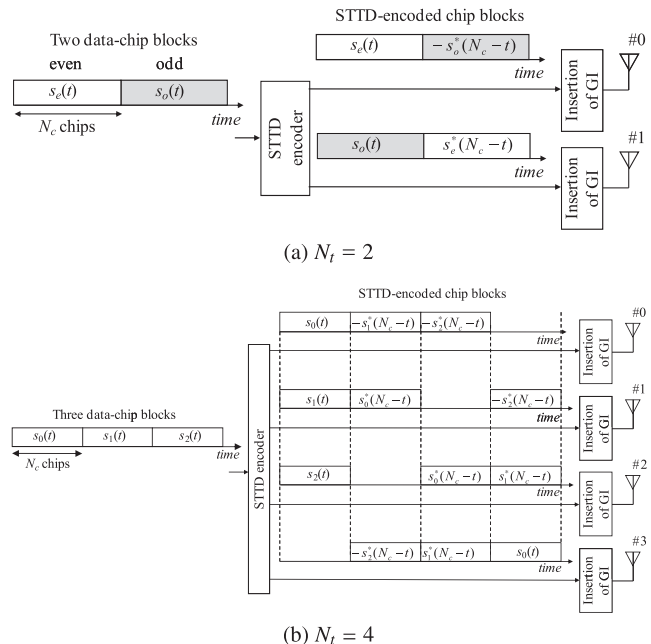


Fig. 3 Time-domain STTD coding.

$\{s_e(t); t = 0 \sim N_c - 1\}$ and $\{s_o(t); t = 0 \sim N_c - 1\}$. Time-domain space-time coding is applied to $\{s_e(t)\}$ and $\{s_o(t)\}$ as shown in Fig. 3 [15]. By applying this encoding, STTD decoding can be performed in frequency-domain together with FDE. After inserting the GI, two consecutive chip blocks are transmitted over a frequency-selective fading channel and received at a receiver. After the GI is removed, the two consecutive received chip blocks $\{r_e(t); t = 0 \sim N_c - 1\}$ and $\{r_o(t); t = 0 \sim N_c - 1\}$ are decomposed into the frequency-domain signals $\{R_e(k); k = 0 \sim N_c - 1\}$ and $\{R_o(k); k = 0 \sim N_c - 1\}$ by applying N_c -point FFT. $R_e(k)$ and $R_o(k)$ are given by

$$\begin{cases} R_e(k) = \sqrt{\frac{2E_c}{N_t T_c}} H_0(k) S_e(k) \\ \quad + \sqrt{\frac{2E_c}{N_t T_c}} H_1(k) S_o(k) + \Pi_e(k) \\ R_o(k) = -\sqrt{\frac{2E_c}{N_t T_c}} H_0(k) S_o^*(k) \\ \quad + \sqrt{\frac{2E_c}{N_t T_c}} H_1(k) S_e^*(k) + \Pi_o(k), \end{cases} \quad (10)$$

where $H_{0(\text{or } 1)}(k)$ and $\Pi_{e(\text{or } o)}(k)$ are the channel gain between the 0th (or 1st) transmit antenna and the receiver and the noise. $H_{0(\text{or } 1)}(k)$ is given by

$$H_{0(\text{or } 1)}(k) = \sum_{l=0}^{L-1} h_{0(\text{or } 1),l} \exp\left(-j2\pi k \frac{\tau_l}{N_c}\right). \quad (11)$$

We assume block fading where the path gains remain constant over two consecutive blocks of $2(N_c + N_g)$ chips. Hence, an index representing odd and even chip blocks is omitted from $h_{0(\text{or } 1),l}$ and $H_{0(\text{or } 1)}(k)$.

Joint MMSE-FDE and STTD decoding is carried out

as follows [15];

$$\begin{cases} \hat{R}_e(k) = R_e(k)W_0^*(k) + R_o^*(k)W_1(k) \\ \hat{R}_o(k) = R_e(k)W_1^*(k) - R_o^*(k)W_0(k), \end{cases} \quad (12)$$

where $W_{0(or1)}(k)$ is the MMSE-FDE weight combined with STTD decoding, which minimizes the mean square error (MSE) between $\hat{R}_{e(or o)}(k)$ and $S_{e(or o)}(k)$. N_c -point IFFT is applied to $\{\hat{R}_e(k); k = 0 \sim N_c - 1\}$ and $\{\hat{R}_o(k); k = 0 \sim N_c - 1\}$ to obtain the equalized and STTD decoded time-domain chip blocks, $\{\tilde{r}_e(t); t = 0 \sim N_c - 1\}$ and $\{\tilde{r}_o(t); t = 0 \sim N_c - 1\}$. Finally, despreading (see Eq. (9)) is done before data demodulation.

4. Residual ICI after MMSE-FDE

The residual ICI after MMSE-FDE, denoted by $\{M_{CD}(k); k = 0 \sim N_c - 1\}$ for CDTD and $\{M_{e(or o)}(k); k = 0 \sim N_c - 1\}$ for STTD, can be written as [9]

$$\begin{cases} M_{CD}(k) = \sqrt{\frac{2E_c}{N_t T_c}} \left\{ \hat{H}_{CD}(k) - \left(\frac{1}{N_c} \sum_{k'=0}^{N_c-1} \hat{H}_{CD}(k') \right) \right\} \\ \quad \times S(k) \quad \text{for CDTD} \\ M_{e(or o)}(k) = \sqrt{\frac{2E_c}{N_t T_c}} \left\{ \hat{H}_{ST}(k) - \left(\frac{1}{N_c} \sum_{k'=0}^{N_c-1} \hat{H}_{ST}(k') \right) \right\} \\ \quad \times S_{e(or o)}(k) \quad \text{for STTD,} \end{cases} \quad (13)$$

where $\hat{H}_{ST}(k)$ is the equivalent channel gain after joint MMSE-FDE and STTD decoding and is given by

$$\hat{H}_{ST}(k) = W_0(k)H_0^*(k) + W_1(k)H_1^*(k) \quad \text{for STTD.} \quad (14)$$

$M_{CD}(k)$ and $M_e(k)$ are shown in Fig. 4 for an $L = 16$ path frequency-selective fading channel when $N_c = 256$ and $E_b/N_0 = 10$ dB. CDTD enhances the frequency-selectivity of the channel and hence, the large ICI is produced after MMSE-FDE. However, STTD produces less residual ICI since the frequency-selectivity can be suppressed by antenna diversity effect obtained through STTD decoding.

5. ICI Cancellation

To reduce the residual ICI after MMSE-FDE and improve the BER performance using CDTD and STTD, frequency-domain ICI cancellation is introduced [9]. A DS-CDMA receiver using joint MMSE-FDE and frequency-domain ICI cancellation is shown in Fig. 5. In this section, the process in the i th iteration is described.

5.1 Joint MMSE-FDE and ICI Cancellation

5.1.1 CDTD

MMSE-FDE is carried out as

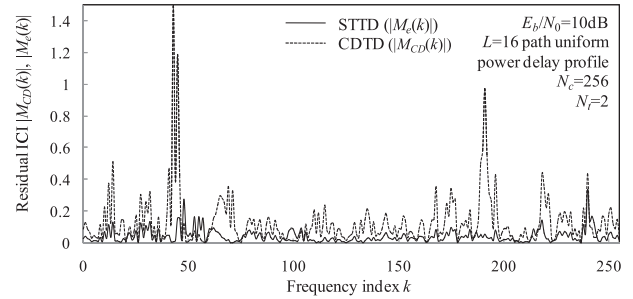


Fig. 4 Frequency spectrum of residual ICI.

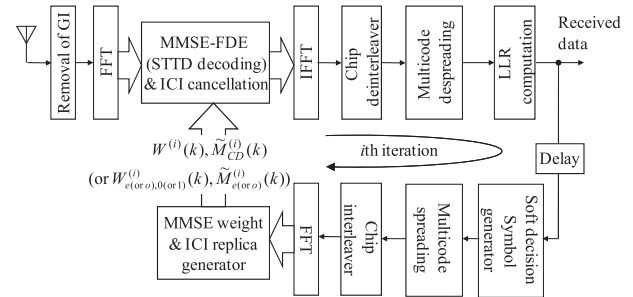


Fig. 5 DS-CDMA receiver using joint MMSE-FDE and ICI cancellation.

$$\hat{R}^{(i)}(k) = R(k)W^{(i)}(k), \quad (15)$$

where $W^{(i)}(k)$ is the MMSE-FDE weight, taking into account the residual ICI, at the i th iteration. $W^{(i)}(k)$ is given by [9]

$$W^{(i)}(k) = \frac{H_{CD}^*(k)}{\rho^{(i-1)} |H_{CD}(k)|^2 + \left(\frac{1}{N_t} \frac{U}{SF} \frac{E_s}{N_0} \right)^{-1}}, \quad (16)$$

where $\rho^{(i-1)}$ ($0 \leq \rho^{(i-1)} \leq 1$) shows the extent to which the residual ICI remains and is given as

$$\rho^{(i-1)} = \frac{1}{U} \frac{SF}{N_c} \sum_{m=0}^{N_c/SF-1} \sum_{u=0}^{U-1} \left\{ E[|d_u(m)|^2] - |\tilde{d}_u^{(i-1)}(m)|^2 \right\} \quad (17)$$

with $\rho^{(-1)} = 1$ and $\{\tilde{d}_u^{(i-1)}(m); m = 0 \sim N_c/SF - 1\}$ being the soft replica of the transmitted symbol block $\{d_u(m)\}$. $E[|d_u(m)|^2]$ is the expectation of $|d_u(m)|^2$ for the given received chip block and $E[|d_u(m)|^2] = 1$ always if QPSK data modulation is used. Note that $\rho^{(i-1)} \approx 1$ (i.e., $|\tilde{d}_u^{(i-1)}(m)|^2 \approx 0$) means the residual ICI is kept intact, while $\rho^{(i-1)} \approx 0$ (i.e., $|\tilde{d}_u^{(i-1)}(m)|^2 \approx 1$) means the residual ICI is sufficiently reduced.

ICI cancellation is performed on $\hat{R}^{(i)}(k)$ as

$$\tilde{R}^{(i)}(k) = \hat{R}^{(i)}(k) - \tilde{M}_{CD}^{(i)}(k), \quad (18)$$

where $\tilde{M}_{CD}^{(i)}(k)$ is the replica of $M_{CD}(k)$, and is given from Eq. (13), by

$$\tilde{M}_{CD}^{(i)}(k) = \begin{cases} 0 & \text{for } i = 0 \\ \sqrt{\frac{2E_c}{N_t T_c}} \left\{ \hat{H}_{CD}^{(i)}(k) - \left(\frac{1}{N_c} \sum_{k'=0}^{N_c-1} \hat{H}_{CD}^{(i)}(k') \right) \right\} \\ \times \tilde{S}^{(i-1)}(k) & \text{for } i > 0, \end{cases} \quad (19)$$

where $\hat{H}_{CD}^{(i)}(k) = W^{(i)}(k)H_{CD}(k)$ is the equivalent channel gain after MMSE-FDE at the i th iteration and $\{\tilde{S}^{(i-1)}(k); k = 0 \sim N_c - 1\}$ is the replica of $S(k)$. After ICI cancellation is done, N_c -point IFFT is applied to obtain the equalized chip block $\{\tilde{r}^{(i)}(t); t = 0 \sim N_c - 1\}$. Finally, despreading is carried out on $\{\tilde{r}^{(i)}(t)\}$ to get the decision variable $\{\tilde{d}_u^{(i)}(m); m = 0 \sim N_c/SF - 1\}$ associated with $d_u(m)$.

5.1.2 STTD

Joint MMSE-FDE and STTD decoding is performed using $R_e(k)$ and $R_o(k)$ as

$$\begin{cases} \hat{R}_e^{(i)}(k) = R_e(k)W_{e,0}^{(i)*}(k) + R_o^*(k)W_{e,1}^{(i)}(k) \\ \hat{R}_o^{(i)}(k) = R_e(k)W_{o,1}^{(i)*}(k) - R_o^*(k)W_{o,0}^{(i)}(k), \end{cases} \quad (20)$$

where $W_{e(or o), 0(or 1)}^{(i)}(k)$ is the MMSE-FDE weight combined with STTD decoding, which takes into account the residual ICI. $W_{e(or o), 0(or 1)}^{(i)}(k)$ is given by

$$\begin{aligned} W_{e(or o), 0(or 1)}^{(i)}(k) &= \frac{H_{0(or 1)}(k)}{\rho_{e(or o)}^{(i-1)} (|H_0(k)|^2 + |H_1(k)|^2) + \left(\frac{1}{N_t} \frac{U}{SF} \frac{E_s}{N_0} \right)^{-1}}, \\ &\quad (21) \end{aligned}$$

with

$$\rho_{e(or o)}^{(i-1)} = \frac{1}{U} \frac{SF}{N_c} \sum_{m=0}^{N_c/SF-1} \sum_{u=0}^{U-1} \left\{ E[|d_{e(or o), u}(m)|^2] - \left| \tilde{d}_{e(or o), u}^{(i-1)}(m) \right|^2 \right\}, \quad (22)$$

where $\rho_{e(or o)}^{(-1)} = 1$ and $\{\tilde{d}_{e(or o), u}^{(i-1)}(m); m = 0 \sim N_c/SF - 1\}$ is the replica of the transmitted symbol block $\{d_{e(or o), u}(m)\}$. $E[|d_{e(or o), u}(m)|^2]$ is the expectation of $|d_{e(or o), u}(m)|^2$ for the given received chip block and $E[|d_{e(or o), u}(m)|^2] = 1$ always if QPSK data modulation is used. ICI cancellation is done for $\hat{R}_{e(or o)}^{(i)}(k)$ as

$$\hat{R}_{e(or o)}^{(i)}(k) = \hat{R}_{e(or o)}^{(i)}(k) - \tilde{M}_{e(or o)}^{(i)}(k), \quad (23)$$

where $\tilde{M}_{e(or o)}^{(i)}(k)$ is the replica of $M_{e(or o)}(k)$, and is given from Eq. (13), by

$$\tilde{M}_{e(or o)}^{(i)}(k) = \begin{cases} 0 & \text{for } i = 0 \\ \sqrt{\frac{2E_c}{N_t T_c}} \left\{ \hat{H}_{e(or o)}^{(i)}(k) - \left(\frac{1}{N_c} \sum_{k'=0}^{N_c-1} \hat{H}_{e(or o)}^{(i)}(k') \right) \right\} \\ \times \tilde{S}_{e(or o)}^{(i-1)}(k) & \text{for } i > 0, \end{cases} \quad (24)$$

where $\hat{H}_{e(or o)}^{(i)}(k) = W_{e(or o), 0}^{(i)}H_0^*(k) + W_{e(or o), 1}^{(i)}H_1^*(k)$ is the equivalent channel gain after joint MMSE-FDE and STTD decoding at the i th iteration. $\tilde{S}_{e(or o)}^{(i-1)}(k)$ is the replica of $S_{e(or o)}(k)$. After ICI cancellation, N_c -point IFFT is applied to obtain the chip block $\{\tilde{r}_{e(or o)}^{(i)}(t); t = 0 \sim N_c - 1\}$. Finally, despreading is carried out to obtain the decision variable $\{\tilde{d}_{e(or o), u}^{(i)}(m); m = 0 \sim N_c/SF - 1\}$ associated with $\{d_{e(or o), u}(m)\}$.

5.2 ICI Replica Generation

For the case of CDTD, using the decision variable $\tilde{d}_u^{(i-1)}(m)$ at the $(i-1)$ th iteration stage (see Eq. (9)), the log-likelihood ratio (LLR) $\{L_u(x, m); x = 0 \sim \log_2 K - 1 \text{ and } m = 0 \sim N_c/SF - 1\}$ for the x th bit in the m th symbol $d_u(m)$ ($m = 0 \sim N_c/SF - 1$), where $x = 0 \sim \log_2 K - 1$ and K is the modulation level, is computed using [16]

$$\begin{aligned} L_u(x, m) &= \ln \left(\frac{p^{(i-1)}(b_{x,m} = 1)}{p^{(i-1)}(b_{x,m} = 0)} \right) \\ &\approx \frac{\left| \tilde{d}_u^{(i-1)}(m) - \sqrt{\frac{2E_c}{N_t T_c}} \left(\frac{1}{N_c} \sum_{k=0}^{N_c-1} \hat{H}_{CD}^{(i-1)}(k) \right) d_{b_{x,m}=0}^{\min} \right|^2}{2\hat{\sigma}^2} \\ &\quad - \frac{\left| \tilde{d}_u^{(i-1)}(m) - \sqrt{\frac{2E_c}{N_t T_c}} \left(\frac{1}{N_c} \sum_{k=0}^{N_c-1} \hat{H}_{CD}^{(i-1)}(k) \right) d_{b_{x,m}=1}^{\min} \right|^2}{2\hat{\sigma}^2}, \end{aligned} \quad (25)$$

where $p^{(i-1)}(b_{x,m} = 1)$ and $p^{(i-1)}(b_{x,m} = 0)$ are the *a-posteriori* probabilities of the transmitted bit $b_{x,m}$ being $b_{x,m} = 1$ and $b_{x,m} = 0$, respectively, obtained at the $(i-1)$ th iteration stage. $d_{b_{x,m}=0}^{\min}$ (or $d_{b_{x,m}=1}^{\min}$) is the most probable symbol that gives the minimum Euclidean distance from $\tilde{d}_u^{(i-1)}(m)$ among all candidate symbols with $b_{x,m} = 0$ (or 1). $2\hat{\sigma}^2$ is the variance of the noise plus residual ICI.

For QPSK data modulation, using $L_u(0, m)$ and $L_u(1, m)$, the soft symbol replica is obtained as

$$\tilde{d}_u^{(i-1)}(m) = \frac{1}{\sqrt{2}} \tanh \left(\frac{L_u(0, m)}{2} \right) + j \frac{1}{\sqrt{2}} \tanh \left(\frac{L_u(1, m)}{2} \right). \quad (26)$$

Using $\tilde{d}_u^{(i-1)}(m)$, $\rho_{e(or o)}^{(i-1)}$ of Eq. (17) can be computed for updating the MMSE-FDE weight $W^{(i)}(k)$ for the i th iteration.

Then, $\tilde{d}_u^{(i-1)}(m)$ is spread and code-multiplexed to generate the chip block replica $\{\tilde{s}^{(i-1)}(t); t = 0 \sim N_c - 1\}$. After

applying N_c -point FFT to $\{\tilde{s}^{(i-1)}(t)\}$, the frequency-domain signal replica $\{\tilde{S}^{(i-1)}(k); k = 0 \sim N_c - 1\}$ is obtained, which is used for generating the ICI replica of Eq. (19).

For the case of STTD, the above process is done for the two consecutive blocks to compute $\rho_{e(\text{or } o)}^{(i-1)}$ of Eq. (22) and $\tilde{S}_{e(\text{or } o)}^{(i-1)}(k)$ in Eq. (24).

6. SNR for Perfect ICI Cancellation

The BER lower-bound achievable with perfect ICI cancellation for CDTD and STTD can be derived using the signal-to-noise power ratio (SNR). Below, the SNR expression is derived assuming the perfect ICI cancellation (i.e., $\tilde{d}_u^{(i-1)}(m) = d_u(m)$ and $\tilde{S}^{(i-1)}(k) = S(k)$ for CDTD, while $\tilde{d}_{e(\text{or } o),u}^{(i-1)}(m) = d_{e(\text{or } o),u}(m)$ and $\tilde{S}_{e(\text{or } o)}^{(i-1)}(k) = S_{e(\text{or } o)}(k)$ for STTD). Since $\rho^{(i)} = 0$ and $\rho_{e(\text{or } o)}^{(i)} = 0$ from Eqs. (17) and (22), MMSE-FDE weight is the same as the maximum ratio combining (MRC) weight given by [17]

$$\begin{cases} W^{(i)}(k) = H_{CD}^*(k) & \text{for CDTD} \\ W_{e,0(\text{or } 1)}^{(i)}(k) = H_{0(\text{or } 1)}(k) & \text{for STTD,} \end{cases} \quad (27)$$

where the weight for the even block is only considered for STTD. Using Eqs. (4), (15), (18), (19) and (27) for CDTD and Eqs. (10), (20), (23), (24) and (27) for STTD, the frequency-domain signals $\tilde{R}(k)$ for CDTD and $\tilde{R}_e(k)$ for STTD with perfect ICI cancellation are respectively given by

$$\begin{cases} \tilde{R}(k) = \sqrt{\frac{2E_c}{N_t T_c}} \left(\frac{1}{N_c} \sum_{k'=0}^{N_c-1} |H_{CD}(k')|^2 \right) S(k) \\ \quad + H_{CD}^*(k) \Pi(k) & \text{for CDTD} \\ \tilde{R}_e(k) = \sqrt{\frac{2E_c}{N_t T_c}} \left(\frac{1}{N_c} \sum_{k'=0}^{N_c-1} (|H_0(k')|^2 + |H_1(k')|^2) \right) S_e(k) \\ \quad + H_0^*(k) \Pi_e(k) + H_1^*(k) \Pi_o(k) & \text{for STTD,} \end{cases} \quad (28)$$

The SNR after despreading, denoted by γ_{CD} and γ_{ST} respectively for CDTD and for STTD, is given by [17]

$$\begin{cases} \gamma_{CD} = \frac{2E_s}{N_0} \left(\frac{1}{N_t} \frac{1}{N_c} \sum_{k=0}^{N_c-1} |H_{CD}(k)|^2 \right) & \text{for CDTD} \\ \gamma_{ST} = \frac{2E_s}{N_0} \left(\frac{1}{N_t} \frac{1}{N_c} \sum_{k=0}^{N_c-1} |H_0(k)|^2 + |H_1(k)|^2 \right) & \text{for STTD,} \end{cases} \quad (29)$$

where E_s/N_0 is the symbol energy-to-AWGN power spectrum density ratio. Substituting Eqs. (5) and (11) into (29) gives

$$\gamma_{CD} = \gamma_{ST} = \frac{2E_s}{N_0} \left(\frac{1}{N_t} \sum_{n=0}^{N_t-1} \sum_{l=0}^{L-1} |h_{n,l}|^2 \right) \quad \text{for CDTD and STTD.} \quad (30)$$

The same SNR can be achieved for CDTD and STTD if

the residual ICI is perfectly cancelled. It can be seen from Eqs. (29) and (30) that the frequency diversity gain achieved by CDTD is equivalent to the frequency diversity gain plus antenna diversity gain achieved by STTD.

Assuming quaternary phase shift keying (QPSK) data-modulation, the conditional BER for the given set of $\{h_{n,l}; n = 0 \sim N_t - 1 \text{ and } l = 0 \sim L - 1\}$ is given by

$$p_b \left(\frac{E_s}{N_0}, \{h_{n,l}\} \right) = \frac{1}{2} \text{erfc} \left[\sqrt{\frac{1}{4} \gamma_{CD(\text{or } ST)}} \right], \quad (31)$$

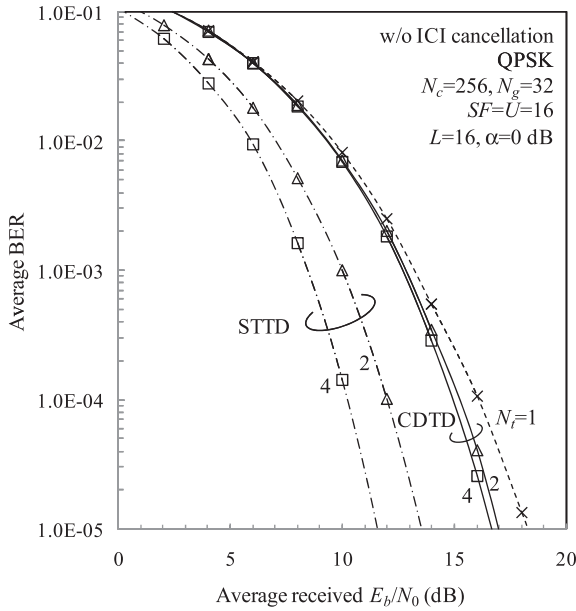
where $\text{erfc}[x] = (2/\sqrt{\pi}) \int_x^\infty \exp(-t^2) dt$ is the complementary error function. The BER lower-bound can be numerically evaluated by averaging Eq. (31) over all realizations of $\{h_{n,l}; n = 0 \sim N_t - 1 \text{ and } l = 0 \sim L - 1\}$.

7. Computer Simulation

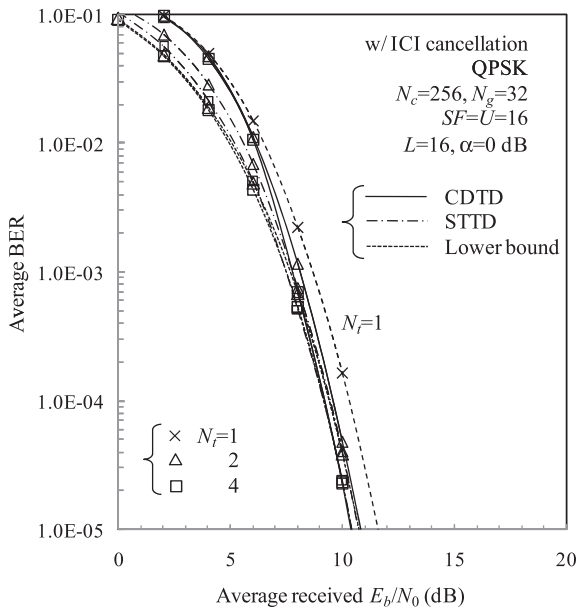
We assume QPSK data-modulation, $N_c = 256$ chips, $N_g = 32$ chips. The channel is assumed to be a frequency-selective block Rayleigh fading channel having a chip-spaced $L = 16$ -path exponential power delay profile with decay factor α (dB). Perfect chip timing and ideal channel estimation are assumed. The number of iterations of joint MMSE-FDE and ICI cancellation is set to $i = 3$, which provides sufficiently improved BER performance.

The simulated BER performance of DS-CDMA with MMSE-FDE is plotted in Fig. 6 as a function of the average received bit energy-to-AWGN power spectrum density ratio E_b/N_0 , defined as $E_b/N_0 = 0.5SF(E_c/N_0)(1 + N_g/N_c)$ when $\alpha = 0$ dB (i.e., uniform power delay profile). The BER performance is plotted for CDTD, STTD and $N_t = 1$ (i.e., no antenna diversity). For CDTD, a cyclic delay of $\Delta = 32$ -chip is used [12]. For STTD using $N_t = 4$, space-time coding with a coding rate of 3/4 is used [18]. We assume the spreading factor $SF = 16$ and $U = SF$, i.e., full code-multiplexing. For comparison, the BER performance without ICI cancellation is also plotted in Fig. 6(a). We first discuss the case without ICI cancellation. When $\alpha = 0$ dB, since the channel frequency-selectivity is sufficiently strong, CDTD provides only a slight performance improvement. STTD performs better than CDTD since it can suppress the frequency-selectivity (thereby reducing the residual ICI) by the antenna diversity gain obtained through space-time encoding and decoding. When $N_t = 4$, the difference in the required E_b/N_0 between CDTD and STTD for BER = 10^{-4} is 4.7 dB. This gap is mainly due to the residual ICI.

The use of ICI cancellation can significantly improve the BER performances as seen from Fig. 6(b). The BER lower-bound computed using Eqs. (30) and (31) is also plotted. CDTD produces large residual ICI. The use of ICI cancellation significantly improves the BER performance of CDTD and provides almost the same BER performance for CDTD and STTD as anticipated in Sect. 6. However, a slight performance difference between CDTD and STTD can be seen in a low E_b/N_0 region. This is because the decision



(a) Without ICI cancellation.

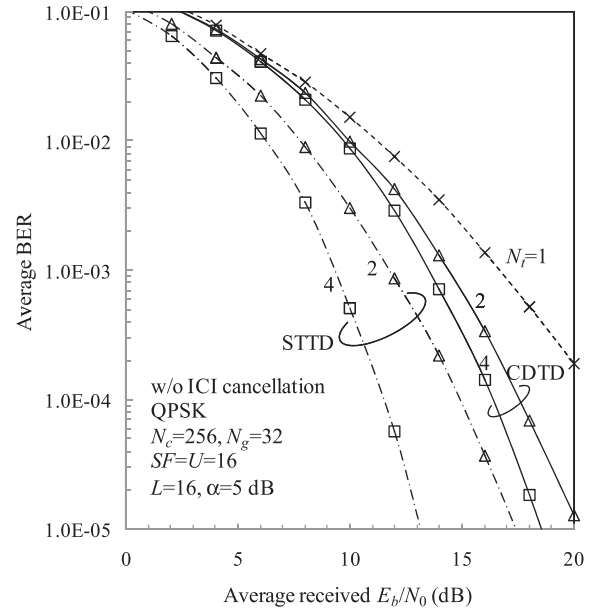


(b) With ICI cancellation.

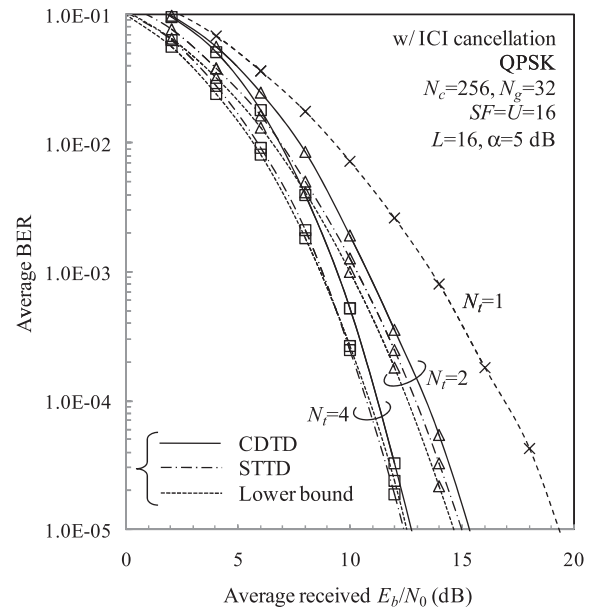
Fig. 6 Simulated BER performance of DS-CDMA/MMSE-FDE ($\alpha = 0$ dB).

variables obtained at $i = 0$ are more erroneous for CDTD than for STTD as seen from Fig. 6(a) and hence, the accuracy of the soft symbol replica is worse for CDTD than for STTD. In a high E_b/N_0 region, however, both CDTD and STTD give almost the same BER performance as the lower-bound. Note that, when $\alpha = 0$ dB, since the channel frequency-selectivity is sufficiently strong and the frequency diversity gain can be achieved by FDE, only a slight performance improvement can be achieved by the additional use of CDTD or STTD.

The simulated BER performance of DS-CDMA with MMSE-FDE and CDTD (or STTD) is plotted in Fig. 7 when



(a) Without ICI cancellation.



(b) With ICI cancellation.

Fig. 7 Simulated BER performance of DS-CDMA/MMSE-FDE ($\alpha = 5$ dB).

$\alpha = 5$ dB. Figure 7(a) shows the BER performance without ICI cancellation. When $\alpha = 5$ dB (weak frequency-selective channel), the frequency diversity gain is smaller and hence the BER performance is worse than when $\alpha = 0$ dB (strong frequency-selective channel). In such a weak frequency-selective channel, CDTD is effective to improve the BER performance. However, the BER performance with CDTD is still inferior to that using STTD which can achieve the antenna diversity gain.

Figure 7(b) shows the simulated BER performance with ICI cancellation. The BER lower-bound computed using Eqs. (30) and (31) is also plotted for comparison. The

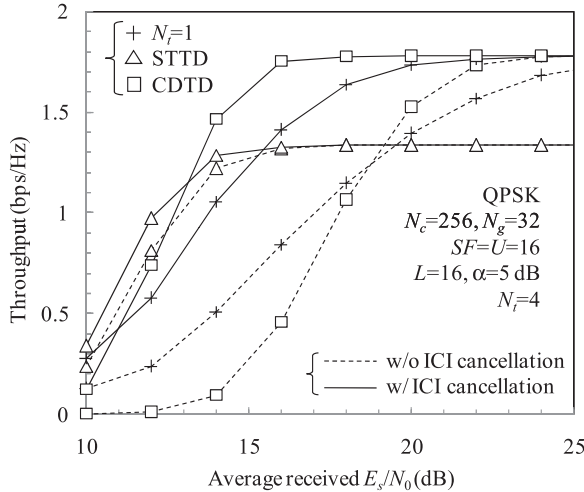


Fig. 8 Simulated throughput of DS-CDMA/MMSE-FDE.

use of ICI cancellation can significantly improve the BER performance. Since the frequency diversity gain achievable by FDE is smaller when $\alpha = 5$ dB, the performance improvement from $N_t = 1$ is due to the antenna diversity gain achieved by space-time encoding/decoding for STTD and due to the additional frequency diversity gain achieved by the enhancement of the frequency-selectivity for CDTD. Also seen is that CDTD provides a performance only slightly inferior to STTD (the reason for which has been given when we discussed the results shown in Fig. 6) and both CDTD and STTD give the performance very close to the lower-bound. With STTD (CDTD) using $N_t = 4$, the E_b/N_0 reduction from the single transmit antenna case ($N_t = 1$) is 6 (5.5) dB for $\text{BER} = 10^{-4}$.

Figure 8 plots the throughputs of DS-CDMA using MMSE-FDE when CDTD and STTD both with $N_t = 4$ are applied. For comparison, the throughput of no transmit diversity ($N_t = 1$) is also plotted. The throughput S is given as

$$S = R(\log_2 K)(1 - \text{PER}) \left(\frac{1}{1 + N_g/N_c} \right). \quad (32)$$

where $R = 1$ for CDTD and $R = 3/4$ for STTD when $N_t = 4$, K is the modulation level, PER is the packet error rate. The maximum throughput is 1.78 bit/s/Hz for CDTD ($R = 1$) while it is 1.33 bit/s/Hz for STTD ($R = 3/4$) when $K = 4$ (QPSK modulation), $N_c = 256$, and $N_g = 32$. Without ICI cancellation, CDTD provides lower throughput than no transmit diversity when $E_s/N_0 \leq 18$ dB. This is because the average equivalent channel gain $(1/N_c) \sum_{k=0}^{N_c-1} \hat{H}_{CD}(k)$ varies more without transmit diversity than with CDTD and therefore, the probability of a packet being received correctly is higher without transmit diversity for a small E_s/N_0 value (note that due to the antenna diversity gain, STTD gives higher throughput than CDTD and no transmit diversity). The throughput degradation of CDTD from STTD is 4.8 ~ 5.2 dB for a throughput range of 0.5 ~ 1 bps/Hz. However, for a high E_s/N_0 region ($E_s/N_0 > 18$ dB), STTD

provides the lowest throughput because of the coding rate $R = 3/4$. The use of ICI cancellation can significantly improve the throughputs of CDTD and no transmit diversity. The throughput of CDTD approaches that of STTD and the E_s/N_0 degradation from STTD is less than 1 dB when $E_s/N_0 < 14$ dB. When $E_s/N_0 > 14$ dB, CDTD gives higher throughput than STTD since the maximum throughput of STTD is reduced because of coding rate $R = 3/4$.

8. Conclusions

In DS-CDMA/MMSE-FDE, STTD provides a better BER performance than CDTD. We showed that the BER performance degradation of CDTD is mainly due to the residual ICI and that the introduction of ICI cancellation gives almost the same BER performance as STTD. This study provided a very important result that CDTD has great advantage of providing a higher throughput than STTD. This was confirmed by computer simulation. When the channel frequency-selectivity is strong enough (i.e., $\alpha = 0$ dB), large frequency diversity gain is obtained; therefore, only a slight additional performance improvement can be achieved by using either CDTD or STTD. However, for a weak frequency-selective channel (i.e., $\alpha = 5$ dB), both CDTD and STTD with ICI cancellation can improve the BER performance significantly. When $N_t = 4$, ICI cancellation can reduce the required E_b/N_0 for $\text{BER} = 10^{-4}$ by as much as 6 dB for STTD and 5.5 dB for CDTD compared to the single transmit antenna case ($N_t = 1$). The throughput was also evaluated by the computer simulation. It was shown that CDTD can achieve higher throughput than STTD when ICI cancellation is introduced.

References

- [1] F. Adachi, "Wireless past and future—Evolving mobile communications systems," IEICE Trans. Fundamentals, vol.E83-A, no.1, pp.55–60, Jan. 2001.
- [2] J.G. Proakis, Digital communications, 2nd ed., McGraw-Hill, 1995.
- [3] F. Adachi, M. Sawahashi, and H. Suda, "Wideband DS-CDMA for next generation mobile communications systems," IEEE Commun. Mag., vol.36, pp.56–69, Sept. 1998.
- [4] F.W. Vook, T.A. Thomas, and K.L. Baum, "Cyclic-prefix CDMA with antenna diversity," Proc. IEEE VTC 2002 Spring, pp.1002–1006, Birmingham, U.S.A., May 2002.
- [5] F. Adachi, T. Sao, and T. Itagaki, "Performance of multicode DS-CDMA using frequency domain equalization in a frequency selective fading channel," Electron. Lett., vol.39, no.2, pp.239–241, Jan. 2003.
- [6] I. Martoyo, G.M.A. Sessler, J. Lubner, and F.K. Jondral, "Comparing equalizers and multiuser detections for DS-CDMA downlink systems," Proc. IEEE VTC 2004-Spring, pp.1649–1653, Milan, Italy, May 2004.
- [7] F. Adachi, D. Garg, S. Takaoka, and K. Takeda, "Broadband CDMA techniques," IEEE Wireless Commun. Mag., vol.12, no.2, pp.8–18, April 2005.
- [8] S. Tomasin and N. Benvenuto, "Equalization and multiuser interference cancellation in CDMA systems," Proc. 6th International Symposium on Wireless Personal Multimedia Communication (WPMC), vol.1, pp.10–14, Yokosuka, Japan, Oct. 2003.
- [9] K. Takeda, K. Ishihara, and F. Adachi, "Downlink DS-CDMA trans-

mission with joint MMSE equalization and ICI cancellation," Proc. IEEE VTC 2006-Spring, vol.4, pp.1762–1766, Melbourne, Australia, May 2006.

- [10] A. Dammann and S. Kaiser, "Standard conformable antenna diversity techniques for OFDM systems and its application to the DVB-T system," Proc. IEEE Globecom, pp.3100–3105, Nov. 2001.
- [11] S.M. Alamouti, "A simple transmit diversity technique for wireless communications," IEEE J. Sel. Areas Commun., vol.16, no.8, pp.1451–1458, Oct. 1998.
- [12] R. Kawauchi, K. Takeda, and F. Adachi, "Space-time cyclic delay transmit diversity for a multi-code DS-CDMA signal with frequency-domain equalization," IEICE Trans. Commun., vol.E90-B, no.3, pp.591–596, March 2007.
- [13] C. Ciochina, D. Castelain, D. Mottier, and H. Sari, "Single-carrier space-frequency block coding: Performance evaluation," 66th IEEE Vehicular Technology Conference (VTC) 2007 Fall, pp.715–719, Baltimore, USA, Sept.–Oct. 2007.
- [14] T.S. Rappaport, Wireless communications, Prentice Hall, 1996.
- [15] K. Takeda, T. Itagaki, and F. Adachi, "Application of space-time transmit diversity to single-carrier transmission with frequency-domain equalization and receive antenna diversity in a frequency-selective fading channel," IEE Proc., Commun., vol.151, no.6, pp.627–632, Dec. 2004.
- [16] A. Stefanov and T. Duman, "Turbo coded modulation for wireless communications with antenna diversity," Proc. IEEE VTC99-Fall, pp.1565–1569, Netherlands, Sept. 1999.
- [17] F. Adachi and K. Takeda, "Bit error rate analysis of DS-CDMA with joint frequency-domain equalization and antenna diversity combining," IEICE Trans. Commun., vol.E87-B, no.10, pp.2991–3002, Oct. 2004.
- [18] W. Su, X.G. Xia, and K.J. R. Liu, "A systematic design of high-rate complex orthogonal space-time block codes," IEEE Commun. Lett., vol.8, no.6, pp.380–382, June 2004.



Fumiyuki Adachi received the B.S. and Dr.Eng. degrees in electrical engineering from Tohoku University, Sendai, Japan, in 1973 and 1984, respectively. In April 1973, he joined the Electrical Communications Laboratories of Nippon Telegraph & Telephone Corporation (now NTT) and conducted various types of research related to digital cellular mobile communications. From July 1992 to December 1999, he was with NTT Mobile Communications Network, Inc. (now NTT DoCoMo, Inc.), where he

led a research group on wideband/broadband CDMA wireless access for IMT-2000 and beyond. Since January 2000, he has been with Tohoku University, Sendai, Japan, where he is a Professor of Electrical and Communication Engineering at the Graduate School of Engineering. His research interests are in CDMA wireless access techniques, equalization, transmit/receive antenna diversity, MIMO, adaptive transmission, and channel coding, with particular application to broadband wireless communications systems. He is a program leader of the 5-year Global COE Program "Center of Education and Research for Information Electronics Systems" (2007–2011), awarded by the Ministry of Education, Culture, Sports, Science and Technology of Japan. From October 1984 to September 1985, he was a United Kingdom SERC Visiting Research Fellow in the Department of Electrical Engineering and Electronics at Liverpool University. He was a co-recipient of the IEICE Transactions best paper of the year award 1996 and again 1998 and also a recipient of Achievement award 2003. He is an IEEE Fellow and was a co-recipient of the IEEE Vehicular Technology Transactions best paper of the year award 1980 and again 1990 and also a recipient of Avant Garde award 2000. He was a recipient of Thomson Scientific Research Front Award 2004 and Ericsson Telecommunications Award 2008.



Kazuaki Takeda received his B.E., M.S. and Dr.Eng. degrees in communications engineering from Tohoku University, Sendai, Japan, in 2003, 2004 and 2007 respectively. Since 2005, he has been a Japan Society for the Promotion of Science (JSPS) research fellow. In 2008, he joined NTT DOCOMO INC. His research interests include equalization, interference cancellation, transmit/receive diversity, and multiple access techniques. He was a recipient of the 2003 IEICE RCS (Radio Communication Systems) Active Research Award and 2004 Inose Scientific Encouragement Prize.



Yohei Kojima received his B.E. degree in communications engineering from Tohoku University, Sendai, Japan, in 2007. Currently he is a graduate student at the Department of Electrical and Communications Engineering, Tohoku University. His research interests include channel estimation and equalization for mobile communication systems.